Fragmentation disrupts the seasonality of Central Amazonian evergreen forests

Authors

Matheus H. Nunes [1, 11], José Luis C. Camargo [2], Grégoire Vincent [3], Kim Calders [4], Rafael S. Oliveira [5], Alfredo Huete [6], Yhasmin Mendes de Moura [7, 8], Bruce Nelson [9], Marielle N. Smith [10], Scott C. Stark [10], Eduardo E. Maeda [1]

[1] Department of Geosciences and Geography, University of Helsinki, Helsinki, 00014, Finland

[2] Biological Dynamics of Forest Fragment Project, National Institute for Amazonian Research, Manaus, AM, 69067-375 Brazil

[3] AMAP, Univ Montpellier, IRD, CIRAD, CNRS, INRAE, Montpellier, France

[4] CAVElab – Computational and Applied Vegetation Ecology, Department of Environment, Faculty of Bioscience Engineering, Ghent University, Ghent, Belgium

[5] Department of Plant Biology, Institute of Biology, University of Campinas, Campinas, Brazil

[6] School of Life Sciences, Faculty of Science, University of Technology Sydney, Sydney, NSW 2007, Australia

[7] Institute of Geography and Geoecology, Karlsruhe Institute of Technology (KIT), Kaiserstr. 12, 76131, Karlsruhe, Germany

[8] Centre for Landscape and Climate Research, School of Geography, Geology and the Environment, University of Leicester, Leicester, LE17RH, United Kingdom

[9] National Institute of Amazonian Research, Manaus, Brazil

[10] Department of Forestry, Michigan State University, East Lansing, MI, USA

[11] Corresponding author (matheus.nunes@helsinki.fi)

Supplementary Information

Supplementary methods 1. Study site and TLS data collection

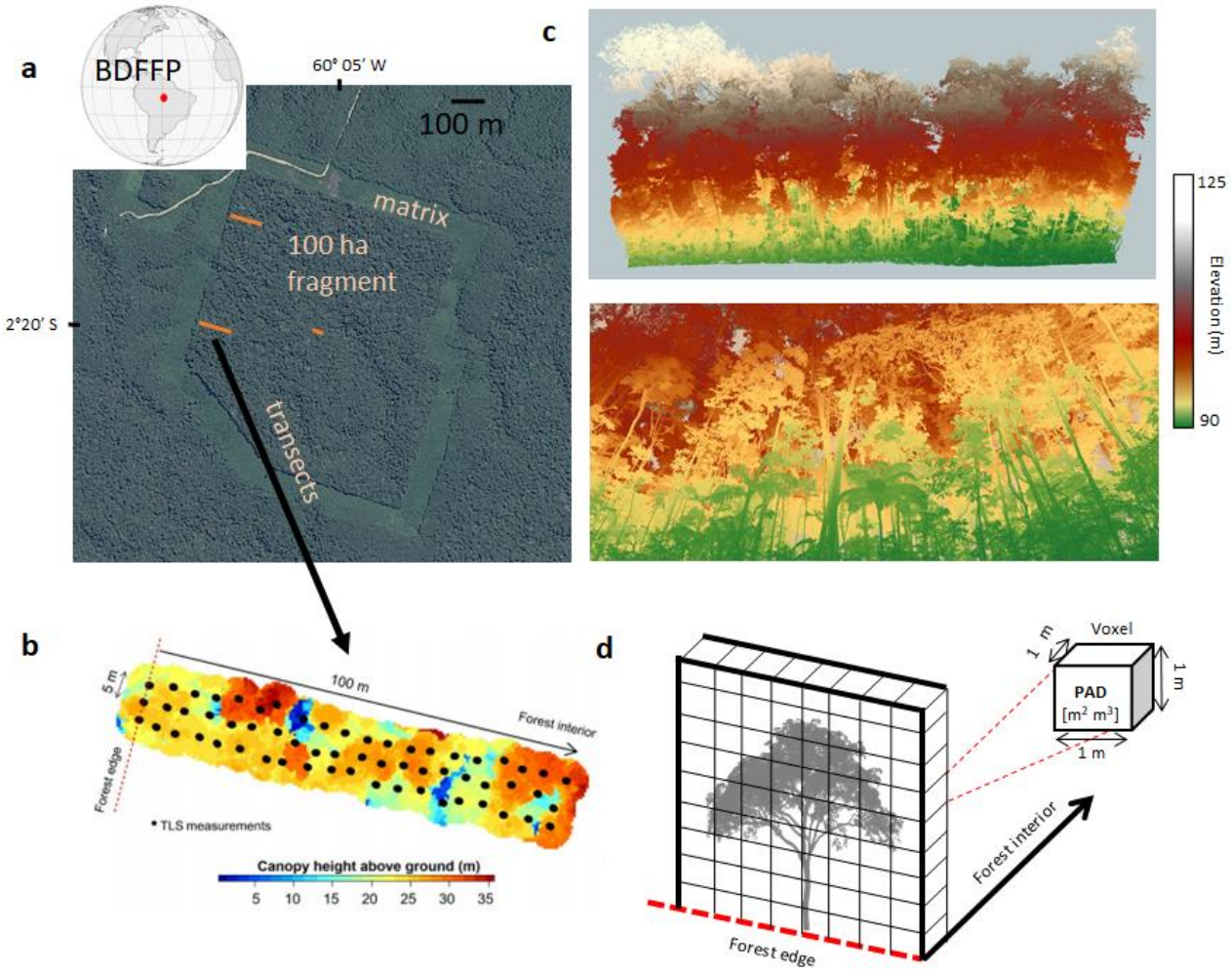

Supplementary Figure 1. a) The Biological Dynamics of Forest Fragments Project (BDFFP), the world's longest-running experimental study of habitat fragmentation, is located in Central Amazonia. The selected 100-ha forest fragment to serve as our experiment is surrounded by a 100 m matrix, regularly cleaned by cutting the regrowth vegetation to keep the forest fragment isolated. Three transects (two of 100 x 10 m at the edges and one of 30 x 10 m at the forest interior) were monitored biweekly between April and October using a terrestrial LiDAR. b) Each transect consisted of three scan lines parallel to each other with scans spaced by 5 m within and between lines. Given that the RIEGL VZ-400i has a zenith angle range of 30–130°, an additional scan was acquired at each sampling location with the scanner tilted at 90° from the vertical position. c) A total of 276 scans

across all transects resulted in a complete sampling of the full hemisphere in each scan location. All scans were later co-registered into a single point cloud per transect. The figures depict a section of a transect's point cloud from a lateral view and from below canopy. d) Plant area density (PAD, m^2 m^{-3}) for all transects were then calculated using a voxel-based approach (with a 5 m buffer around each transect to maximise the PAD data). The volume occupied by vegetation within each transect was divided into 1 m^3 voxels, and the PAD calculated for each of these voxels.

Supplementary methods 2. PAI variation with distance from edges

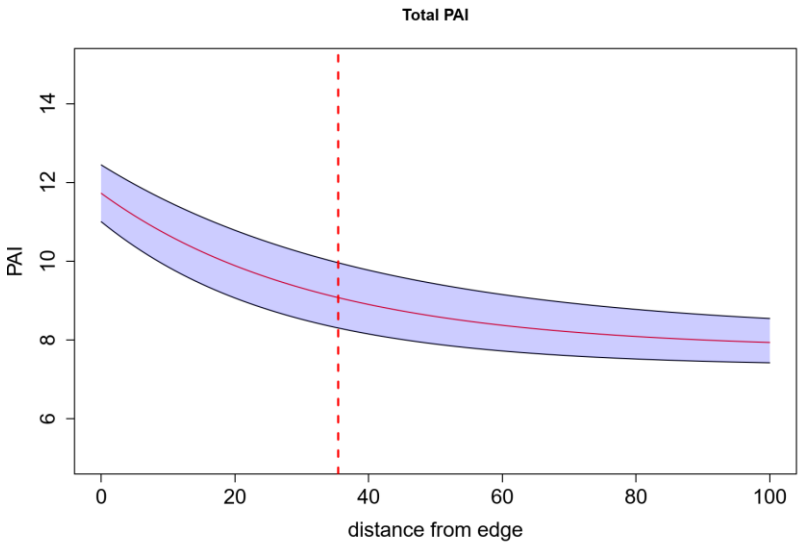

Supplementary Figure 2. Predicted effects of distance from edge (metres) on plant area index (PAI, m^2 m^{-2}), obtained by fitting non-linear mixed models. The solid red curve is the prediction based on parameter values, and the shaded curve corresponding to the 95% confidence intervals. The dashed vertical red line depicts the optimal edge distance threshold fitted a hockey-stick model.

Supplementary methods 3. Vertical PAI variation with distance from edges

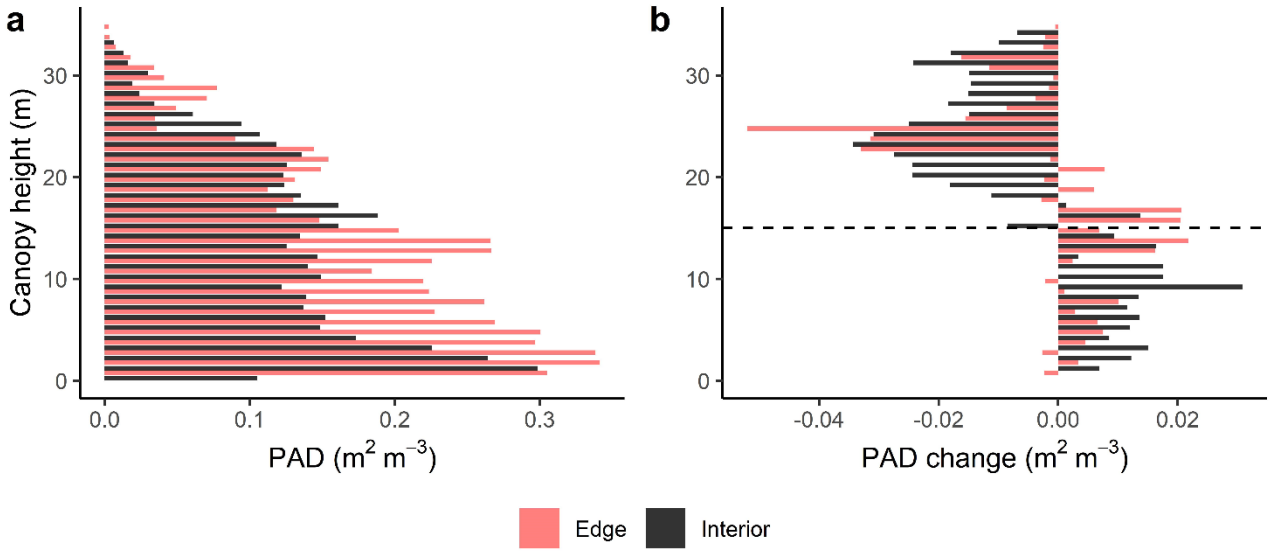

Supplementary Figure 3. a) Mean plant area density (PAD) of forest edges (red) and undisturbed forests in the interior of the fragment (black) per 1-m canopy height. b) PAD changes during the dry season ($PAD_{16th\ October}$ - $PAD_{24th\ June}$) per 1-m canopy height. The dashed horizontal line represents a canopy height threshold of 15 m indicating a shift in PAD change, which was used to separate upper canopy from understory.

Supplementary methods 4. Total PAI for edges and interior

Supplementary Table 1. Results from mixed-effects models (PAI ~ 1 + 1|Transect) taking the non-independence of data from the same transect into account by including a random-effect term 'transect'. We performed χ^2 tests to compare this LME model with other LME models that contained the variables *time*, *edge effects* and an interaction term *time* x *edge effects* to examine the significance of seasonality and fragmentation on PAI variation. χ^2-tests and *P* values were performed by comparing to random-intercept models of the form PAI~ 1 + (1| Transect)) and model explanatory power was assessed in terms of AIC. Models with the lowest AIC and significantly different χ^2 for each stratum was selected (in bold).

Model	**Stratum**	χ^2	Pvalue	AIC
PAI ~ 1	Understory			291263
PAI ~ time	Understory	0	1	291241

PAI ~ *edge effects*	Understory	3705.3	<2e-16 ***	287559
PAI ~ time x *edge effects*	**Understory**	**3713.3**	**<2e-16 *****	**287549**
PAI ~ 1	Upper canopy			202153
PAI ~ time	Upper canopy	0	1	202245
PAI ~ *edge effects*	Upper canopy	116.44	<2e-16 ***	202153
PAI ~ time x *edge effects*	**Upper canopy**	**131.76**	**<2e-16 *****	**202135**
PAI ~ 1	Total			310475
PAI ~ time	Total	0	1	310470
PAI ~ *edge effects*	**Total**	**2298.1**	**<2e-16 *****	**308179**
PAI ~ time x *edge effects*	Total	2301.2	<2e-16 ***	308191

70

71 The most parsimonious model - after comparing all the models using AIC, as well as χ^2 and their
72 corresponding *P* value - to predict PAI for total PAI (without accounting for the vertical stratification)
73 was Eq. 4 (main text). Note that the lack of time effect in Eq. 4 indicated that there is significant
74 temporal variation in only the vertical distribution of PAI (Supplementary Table 1; Supplementary
75 Figure 4a, 4b).

76

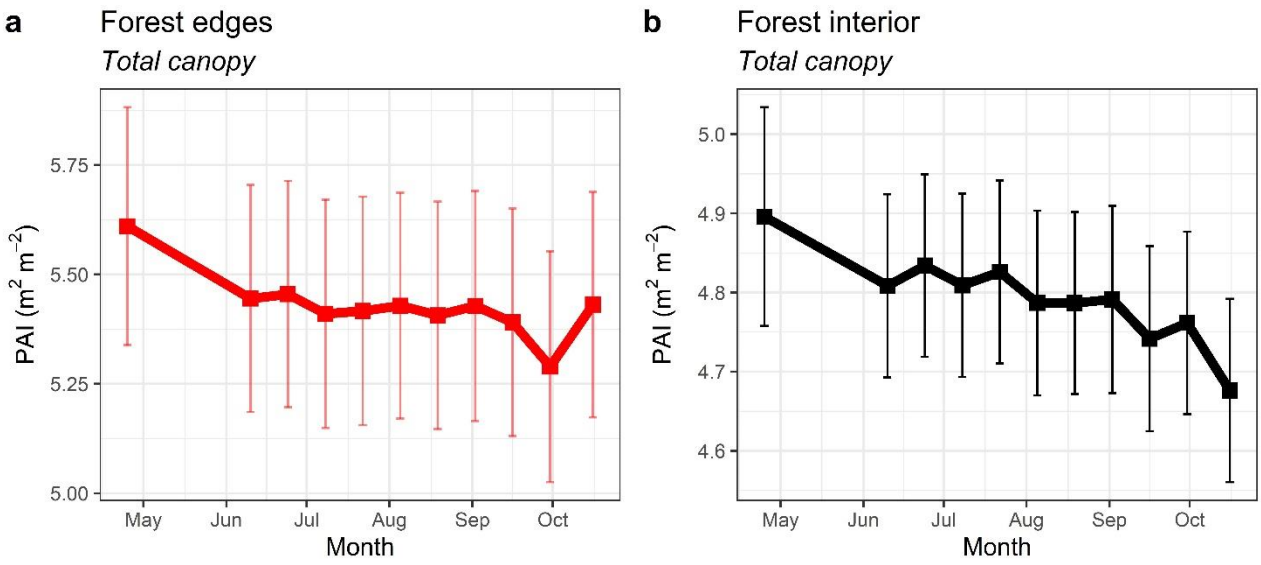

77

78 Supplementary Figure 4. **Plant Area Index time-series.** Plant Area Index for the whole profile of
79 vegetation predicted from linear mixed modelling with date of LiDAR measurements interacting with
80 a categorical variable indicating whether plots were near an edge as fixed variables. Transect was
81 used as a random variable to account for variation between transects of a) forest edges (< 40 m from
82 fragment margins) and b) interior of fragments (≥ 40 m from fragment margins, black). Each point
83 represents the mean values predicted by mixed modelling, with the error bars depicting the
84 bootstrapped 95% confidence intervals.

85

86 **Supplementary methods 5. PAI variation with climatic variables**

87 We also illustrate the significant seasonal variations in PAI against the microclimatic variables
88 measured on the edges of the fragment and in the forest interior. The understory of interior forests
89 had sharp decreases in PAI between April and June (Supplementary Figure 5b), a period when soil
90 moisture was still high, and maximum temperatures were relatively low (27.8 ± 0.64 °C,
91 Supplementary Figure 5d). The understory PAI of these forests increased alongside increases in
92 temperature, and a full recovery in plant area occurred when the temperatures reached the highest
93 values in September.

94

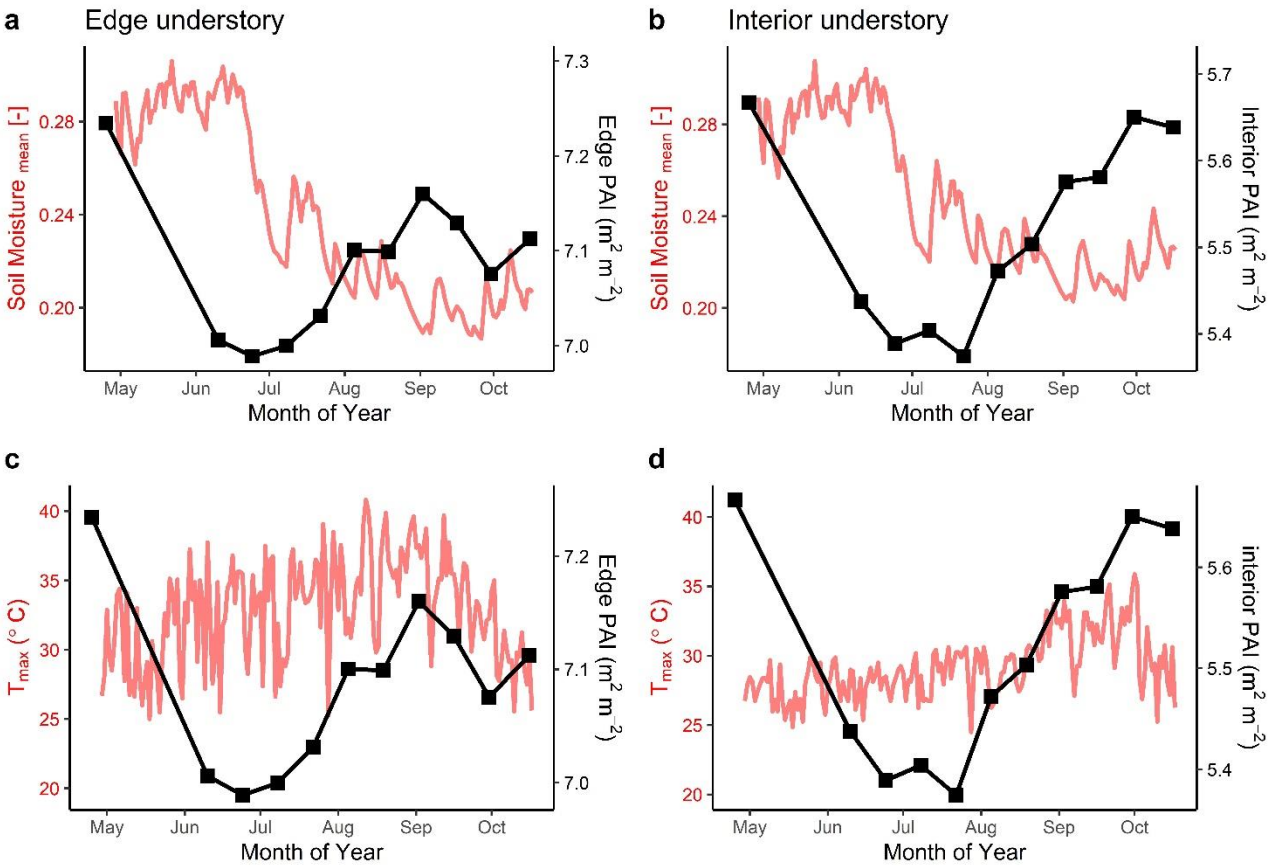

Supplementary Figure 5. Mean daily soil moisture of a) forest edges and b) in the interior of forest fragments. Maximum daily temperatures of c) forest edges and d) in the interior of forest fragments. Microclimate measurements in the understory of these forests were continuously measured every 15 minutes. These microclimatic variables were plotted against the predicted Plant Area Index (PAI) of the understory (< 15 m height) of forest edges and forest interior from Terrestrial Laser Scanning (TLS) measurements. Each black point represents the mean PAI values predicted by mixed modelling.

Both PAI of edges and forest interior were affected, with losses towards the dry season – a period of accumulated monthly precipitation below 200 mm, with significant decreases in soil moisture. The significant decreases in the upper canopy PAI of forest interior in September occurred when temperatures reached the highest temperatures, with some days registering maximum temperatures above 35 °C (Supplementary Figure 6d). The premature loss in upper canopy PAI on forest edges in particular was also synchronised with the very high temperatures above 35 °C during the whole dry

season (Supplementary Figure 6b) – which strongly supports the idea that the seasonal variation of Amazonian forests at the upper canopy level is dependent on water availability and temperature, and that fragmentation exacerbates these effects.

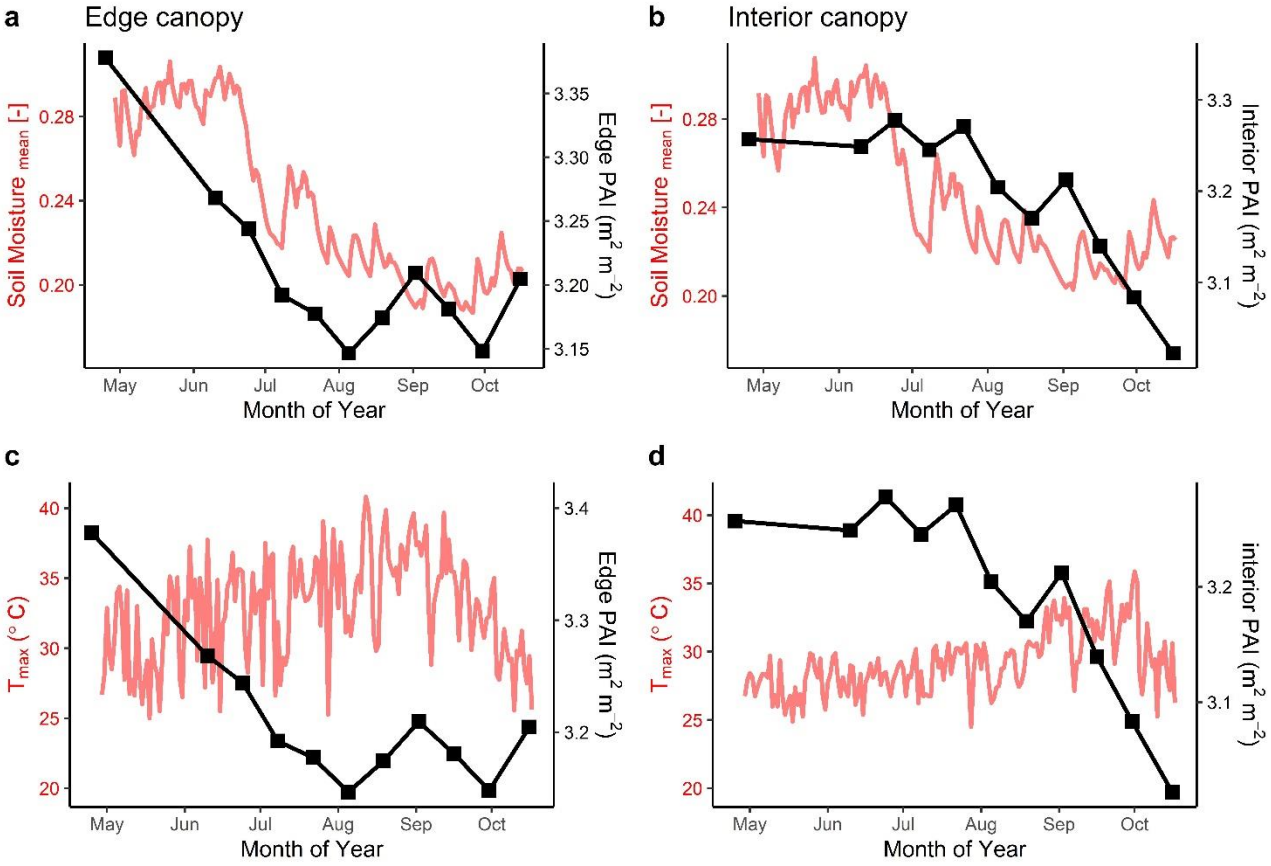

Supplementary Figure 6. Mean daily soil moisture of a) forest edges and b) in the interior of forest fragments. Maximum daily temperatures of c) forest edges and d) in the interior of forest fragments. Microclimate measurements were continuously obtained every 15 minutes. These microclimatic variables were plotted against the predicted Plant Area Index (PAI) of the upper canopy (> 15 m height) of forest edges and forest interior from Terrestrial Laser Scanning (TLS) measurements. Each black point represents the mean PAI values predicted by mixed modelling.